0013-7227/08/$15.00/0
Printed in U.S.A.

Endocrinology 149(4):1666–1677

doi: 10.1210/en.2007-1415

Cysteine-Rich Protein 61 and Connective Tissue Growth Factor Induce Deadhesion and Anoikis of Retinal Pericytes

Haibo Liu, Ru Yang, Babben Tinner, Annam Choudhry, Norbert Schutze, and Brahim Chaqour

Department of Anatomy and Cell Biology (H.L., R.Y., A.C., B.C.), State University of New York Downstate Medical Center, Brooklyn, New York 11203; Health Science Department (B.T.), QBM Cell Science, Ottawa, Canada K1A 0R6; and Orthopedic Center for Musculoskeletal Research (N.S.), University of Würzburg, 97070 Würzburg, Germany

Loss of retinal pericytes is one of the distinctive features of diabetic retinopathy (DR), which is characterized by retinal capillary obliteration. The matricellular proteins, cysteine-rich protein 61 (Cyr61) and connective tissue growth factor (CTGF), are aberrantly expressed in the retinal vasculature from the early stages of DR, but their effects on retinal pericytes are unknown. We show herein that rat retinal pericytes (RRPs) exposed to advanced glycosylation-end products, an important injurious stimulus of diabetes, express increased levels of both Cyr61 and CTGF, and concomitantly undergo anoikis, a form of apoptosis by loss of cell-matrix interactions. Adenovirus-mediated expression of Cyr61 and/or CTGF conferred an anoikis-prone phenotype to rat retinal pericytes, including decreased phosphotyrosine protein levels at focal adhesion points and formation of cortical actin rings. When used as substrates for pericyte attachment and compared with other matrix proteins (*e.g.* type IV collagen), recombinant Cyr61 and CTGF proteins exhibited antiadhesive and apoptogenic activities. Phosphatase inhibitors reversed these effects, suggesting that Cyr61 and CTGF promote dephosphorylation events. Furthermore, Cyr61- and CTGF-induced apoptosis was mediated through the intrinsic pathway and involved the expression of genes that have been functionally grouped as p53 target genes. Expression of the matrix metalloproteinase-2 gene, a known target of p53, was increased in pericytes overexpressing either Cyr61 or CTGF. Inhibition of matrix metalloproteinase-2 had, at least in part, a protective effect against Cyr61- and CTGF-induced apoptosis. Taken together, these findings support the involvement of Cyr61 and CTGF in pericyte detachment and anoikis, implicating these proteins in the pathogenesis of DR. (*Endocrinology* 149: 1666–1677, 2008)

THE CYSTEINE-RICH PROTEIN 61 (Cyr61) and connective tissue growth factor (CTGF), also known as CCN1 and CCN2, respectively, belong to a subset of extracellular matrix (ECM) molecules termed matricellular proteins, which exhibit highly regulated expression during development and in pathological events (1, 2). These immediate early gene-encoded proteins are induced by and modulate, at least in part, the activity of growth factors, hormones, and mechanical forces (3, 4). Structurally, the Cyr61 and CTGF proteins share 40–50% amino acid homology with one another and contain, each, four conserved modular domains with sequence similarities to IGF binding proteins, the von Willebrand factor type C repeat, the thrombospondin type I repeat, and a carboxy-terminal domain containing a cystine-knot motif (5). These modules contain binding sites for integrins, low-density lipoprotein receptors, transmembrane proteoglycans, growth factor receptors, and/or ECM proteins (6–12). Functionally, the Cyr61 and CTGF proteins act as adaptors and modulators of cell-matrix interactions, although their biological activities are contextual and cell type dependent. Cell exposure to these proteins modulate cell adhesion, migration, proliferation, differentiation, survival, and ECM protein synthesis (13). Through these activities, Cyr61 and CTGF regulate diverse biological processes including angiogenesis, development, fibrosis, and hypertrophy.

Numerous studies have described increased Cyr61 and CTGF protein levels in the microvascular complications of diabetes including diabetic retinopathy (14, 15). CTGF was shown to be expressed in microglia, but its localization shifts to retinal microvascular pericytes in a large subset of diabetic persons (16). Similarly, Cyr61 protein levels markedly increase in retinal blood vessels at the early stages of diabetes and in late stages of vitreoproliferative disorders (17). However, what particular function(s) these proteins manifest in retinal blood vessels is unknown. Existing hypotheses associate the activity of these proteins with ECM remodeling (18, 19). In active ophthalmopathy, Cyr61 was suggested to have a role in both orbital inflammation and adipogenesis and serve as an early marker of ocular diseases (20). Twigg *et al.* (19) and Zhou *et al.*, (21) reported that advanced glycosylation end (AGE) products, a major injurious stimulus asso-

First Published Online January 10, 2008

Abbreviations: Ad-CTGF, Adenovirus of CTGF; Ad-Cyr61, adenovirus of CYR61; Ad-GFP, adenovirus encoding green fluorescent protein; AGE, advanced glycosylation end; Bax, Bcl-2-associated X protein; Bcl2, B-cell LL/lymphoma 2; CT, cycle threshold; CTGF, connective tissue growth factor; Cyr61, cysteine-rich protein 61; DAPI, 4′,6-diamidino-2-phenylindole; ECM, extracellular matrix; EthD-1, ethidium homodimer; FA, focal adhesion; FITC, fluorescein isothiocyanate; GAPDH, glyceraldehyde 3-phosphate dehydrogenase; MMP, matrix metalloproteinase; PTEN, phosphatase and tensin homolog; RRP, rat retinal pericyte; SDS, sodium dodecyl sulfate; TRITC, tetramethyl rhodamine isothiocyanate; TUNEL, terminal deoxynucleotidyl transferase-mediated deoxyuridine triphosphate nick end labeling; VEGF, vascular endothelial growth factor.

***Endocrinology* is published monthly by The Endocrine Society (http://www.endo-society.org), the foremost professional society serving the endocrine community.**

ciated with diabetes, act, in part, through cell-derived CTGF to induce fibronectin and type IV collagen expression in fibroblasts and mesangial cells, respectively. However, the actual biological activities of these proteins in the retinal capillaries are unknown.

One of the distinctive features of the process that leads to diabetic retinopathy is the initial loss of retinal capillary pericytes, which outnumber endothelial cells in the retina more than in any other vascular bed (22). Pericytes are smooth muscle-like cells defined by their perivascular localization within the basement membrane that they produce together with endothelial cells. Their putative functions include maintenance of capillary structure and integrity, regulation of endothelium homeostasis, and capillary diameter and angiogenesis (23). Because of their tissue localization outside the blood retinal barrier, retinal pericytes rely entirely on survival signals derived from their surrounding ECM (24). However, diabetes-induced hyperglycemia and associated toxicities affect both the ECM composition and function leading to accelerated death of retinal pericytes and endothelial cells and the loss of the innate vascular autoregulation characteristic of the early stages of diabetic retinopathy (25, 26). Although both Cyr61 and CTGF have been shown to be up-regulated in the retinal capillaries, their effects on pericytes are still unknown (17, 27). This study identifies Cyr61 and CTGF as antiadhesive molecules initiating retinal pericyte anoikis, a form of apoptosis resulting from loss of cell adhesion and/or cell adhesion-dependent signaling.

Materials and Methods

Reagents

All chemicals were of reagent grade. Caspase inhibitors were purchased from Millipore/Chemicon (San Diego, CA). Pharmacological inhibitors were from Sigma-Aldrich. AGE-BSA and Bcl-2-associated X protein (Bax) and B-cell LL/lymphoma 2 (Bcl2) antibodies were from Biovison (Mountain View, CA). Recombinant CYR61 was produced in baculovirus Sf21 cells and purified as previously described (28). Recombinant CTGF was from Novus Biologicals (Littleton, CO). EHS laminin and type IV collagen were from Invitrogen (Carlsbad, CA). Type I collagen was prepared from rat tail tendon. Anti-Cyr61 and anti-CTGF antibodies were described previously (4). Antipaxillin and antiphosphotyrosine antibodies were from Cell Signaling Inc. (Danvers, MA) The 4′,6-diamidino-2-phenylindole (DAPI), fluorescein isothiocyanate (FITC)-conjugated goat antimouse IgG and tetramethyl rhodamine isothiocyanate (TRITC)-conjugated goat antirabbit IgG antibodies were from Vector Laboratories (Burlingame, CA). TRITC-conjugated phalloidin was from Cytoskeleton Inc. (Denver, CO).

Cell culture and treatment

Rat retinal pericytes (RRPs) were isolated from a pool of Sprague Dawley rat retinas by selective sieving at QBM Cell Science Laboratories (Ottawa, Canada). The cells were plated in 35-mm dishes in predefined pericyte medium containing 2% fetal bovine serum obtained from Cell Biolabs, Inc. (San Diego, CA). RRPs were characterized by immunostaining using NG2 (chondroitin sulfate proteoglycan) and desmin antibodies (Chemicon). These cells grow at a very slow rate and can be passaged only twice.

Cyr61 and CTGF adenoviral vector preparation and utilization

Mouse Cyr61 and CTGF cDNAs were isolated by PCR amplification using DNA templates obtained from American Type Culture Collection (Manassas, VA) and cloned into a shuttle vector. The recombinant adenoviruses, Ad-Cyr61 and Ad-CTGF, were produced by cotransfecting an adenoviral shuttle vector with a viral backbone in which the recombinant cDNA is driven by the cytomegalovirus promoter. Recombinant adenovirus amplification was carried out by Vector Biolabs (Philadelphia, PA). The empty adenovirus, Ad-V, and the adenovirus encoding green fluorescent protein (Ad-GFP) were used as controls for infection. All adenoviruses were replication deficient and used at 20 multiplicity of infection. Cells at 80% confluence were incubated with adenoviral vectors first, in serum-free medium for up to 3 h and then in serum-containing medium. Cells were then incubated in serum-free medium for defined periods of time and then processed for various analyses.

Western immunoblotting and fluorescence microscopy

For Western blot analysis, protein samples (24 μg) were fractioned in a 10% sodium dodecyl sulfate (SDS)-polyacrylamide gel and transferred to nitrocellulose membrane, and Western blot analysis was performed with anti-Cyr61, anti-CTGF, or anti-glyceraldehyde 3-phosphate dehydrogenase (GAPDH) antibodies. Immunodetection was performed using enhanced chemiluminescence (Amersham Biosciences, Piscataway, NJ) according to the manufacturer's recommendations.

For immunocytochemical analyses, cells plated on glass coverslips were fixed in 0.4% formaldehyde-PBS for 20 min and permeabilized in 0.1% Triton X-100 at room temperature for 5 min. For visualization of actin stress fibers, cells were stained with TRITC-phalloidin. For immunodetection of specific proteins, cells were incubated with the indicated primary antibodies overnight at 4 C and then treated with TRITC- or FITC-conjugated secondary antibodies. Coverslips were washed several times in PBS between incubations. Images were acquired using the 1024 MDC laser scanning fluorescence imaging system (Bio-Rad Laboratories, Hercules, CA).

Anoikis and terminal deoxynucleotidyl transferase-mediated deoxyuridine triphosphate nick end labeling (TUNEL) assays

Cells undergoing death by anoikis were identified and quantified using the CytoSelect anoikis assay kit according to the manufacturer's instructions (Cell Bioloab). Briefly, cells to be assayed for anoikis were collected, pelleted by centrifugation, and resuspended in culture medium. Cells (400,000) in suspension were added into either an anchorage-resistant poly-Hema-coated or a control uncoated plate. After a 24-h incubation time at 37 C, ethidium homodimer (EthD-1) was added into each well to detect apoptotic cells. Free Eth-D1 is virtually undetectable before interacting with cell membrane. Fluorescence was measured at 515 and 590 nm using a Fluorolite-1000 plate reader (Dynex Technologies, Chantilly, VA).

TUNEL staining was performed in 35-mm dishes using an *in situ* death detection kit according to the manufacturer's instructions (Roche Molecular Biochemicals, Indianapolis, IN). The percentage of TUNEL-positive cells (relative to total counterstained with DAPI) was determined by counting approximately 200 cells in 10 randomly chosen fields per coverslip for each experiment.

Cell adhesion assay

Microtiter 96-well plates were coated overnight at 4 C with 50 μl/well of substrate, *e.g.* Cyr61, CTGF, laminin, type I or IV collagen, or BSA. The wells were then blocked with 0.5% BSA in PBS (100 μl/well) for 2 h at 37 C. Subconfluent cells were trypsinized, washed, and resuspended in adhesion buffer (Hank's balanced salt solution supplemented with 1 mM $MgCl_2$). An aliquot of the cell suspension (40,000 cells) was first preincubated with a vehicle solution or chemical inhibitors for 30 min and then added to the coated plates in a final volume of 50 μl and allowed to attach at 37 C in a humidified incubator for 30 min. Nonattached cells were removed by two washes with PBS. Attached cells were fixed with 4% paraformaldehyde at room temperature for 10 min and stained for 10 min with crystal violet (5 mg/ml in 2% ethanol). After several washes with water, the wells were dried, and the dye was extracted with 2% SDS for 30 min at room temperature. Adhesion was quantified by measurement of absorbance at 550 nm. Nonspecific cell attachment (attachment to wells coated with BSA) was always less than 5%.

RNA isolation and quantitative analysis of mRNA

Total RNA was extracted from cells using RNAEasy column purification protocol (QIAGEN, Valencia, CA). Quantitative real-time RT-PCR assay was performed to quantify the mRNA levels of numerous genes using TaqMan technology on an Applied Biosystems 7000 sequence detection system (Foster City, CA). Highly specific primers were designed using the Web-based primer design program, Primer3 (Whitehead Institute for Biomedical Research, Cambridge, MA). The forward and reverse primers were: 5′-TGAGCTCCAGCACCATCAAG-3′ and 5′-AGTGCCAGCCTGGTCAAGTG-3′ for Cyr61; 5′-CGCCAACCGCAAGATTG-3′ and 5′-ACGGACCCACCGAAGACA-3′ for CTGF, 5′-TGACGATGAGCTGTGGACTC-3′ and 5′-ACAAGAAGGGGAACTTGCAG-3′ for matrix metalloproteinase (MMP)-2; 5′-ACCCCACTCACATTCTCCAG-3′ and 5′-GCCCATCAAAAGGGATAAAG-3′ for MMP-3; 5′-TACGGGCTCGAAGCAGAC-3′ and 5′-AAAGGCGTGTGCCAGTAGAC-3′ for MMP-9; 5′-ACAGAAGGGGAGCAGAAAGC-3′ and 5′-AGATGTCCACCAG GGTCTCA-3′ for vascular endothelial growth factor (VEGF); 5′-CAGACGGCAACTTCAACTGG-3′ and 5′-CAGCCCATGATGGTTCTGAT-3′ for Bax; 5′-CAGGCAGCCAATAACAGTCA-3′ and 5′-CTCCTCCTCCATCCCTTCAT-3′ for Bcl-2 antagonist of cell death (Bad); 5′-GATTGGGGAATGGGTTGGTAG-3′ and 5′-TGCAGAGTGGAGGAAATGGG-3′ for p53; 5′-GGGACTCGCACTTGCAATA-3′ and 5′-AGTTATGGTGCGCTGACTCC-3′ for GADD45a; 5′-TGTTGTGATGGTGGCTTGAG-3′ and 5′-CTCCTGACCCTTCATCCGTA-3′ for apoptosis inhibitor 2; 5′-GTTGCCTCCTCTCCTTTTCG-3′ and 5′-AGCGTGGAAGATTGTTCAGC-3′ for activating transcription factor 5; and 5′-GAGGCAGACCAGCCTAACAG-3′ and 5′-GGCACTTCAGGGCTTTCTCT-3′ for $p21^{WAF1}$. These primers were designed to span exon-exon junctions so that genomic DNA would not be detected. Primers for α1(IV) collagen and β1-laminin chain were obtained commercially (SuperArray Bioscience Corp., Frederick, MD). The cycling parameters for PCR amplification reactions were: AmpliTaq activation 95 C for 10 min, denaturation 95 C for 15 sec, and annealing/extension 60 C for 1 min (40 cycles). Triplicate CT values were analyzed with Microsoft Excel using the comparative cycle threshold (CT) (hh^{CT}) method as described by the manufacturer (Applied Biosystems). Transcript levels (2^{-hhCT}) were obtained by normalizing to an endogenous reference (18S rRNA).

In-gel zymography

Ten micrograms of proteins, as measured using the Bradford assay (Bio-Rad) from conditioned media were mixed with loading buffer and assayed for MMP activity by gel zymography using gelatin-containing precast gels from Invitrogen according to the manufacturer's instructions. Clear digested regions representing MMPs activity were quantified using a Kodak documentation system (Rochester, NY), and molecular weights were estimated using prestained molecular weight markers.

Pathway-specific microarray gene expression profiling

The Oligo GEArray rat apoptosis system from SuperArray Bioscience was used. The array contains 113 oligonucleotide probes representing genes involved in apoptosis. Side-by-side hybridization experiments determine differential gene expression between two samples. Total RNA from Ad-V and Ad-Cyr61-infected cells subjected to DNase digestion to eliminate genomic DNA contamination was used as a template for RT-PCR. The TrueLabeling-AMP 2.0 linear amplification and labeling kit (Superarray, Frederick, MD) was used to convert total RNA to amplified and biotinylated cRNA, which was then hybridized overnight at 60 C with nylon membrane arrays in a hybridization oven. After washing, arrays were incubated with streptavidin and immunodetection was performed using the chemiluminescence detection kit from Amersham Biotech (Pisataway, NJ). The membranes were dried and exposed to x-ray films. Images were quantified using a data analysis software.

Statistical analysis

Data were expressed as means ± SE. To test differences among several means for significance, a one-way ANOVA with the Newman-Keuls multiple comparison test was used. Where appropriate, *post hoc* unpaired *t* test was used to compare two means/groups, and $P < 0.05$ or < 0.01 were considered significant. Statistical analyses were performed using the Prism software for Windows version 4 (GraphPad Inc., San Diego, CA).

Results

Effects of AGE-BSA on Cyr61 and CTGF gene expression in RRPs

As a basis for establishing the potential involvement of Cyr61 and CTGF in retinal pericyte pathology, we first examined the effects of AGE-BSA on the expression of the Cyr61 and CTGF genes. Cultured RRPs were treated with AGE-BSA (100 μg/ml) for various periods of time and the expression of the Cyr61 and CTGF genes was analyzed by real-time PCR and Western immunoblotting. As shown in (Fig. 1A), AGE-BSA induced nearly 2- and 4-fold increases of either Cyr61 or CTGF mRNA levels after incubation with

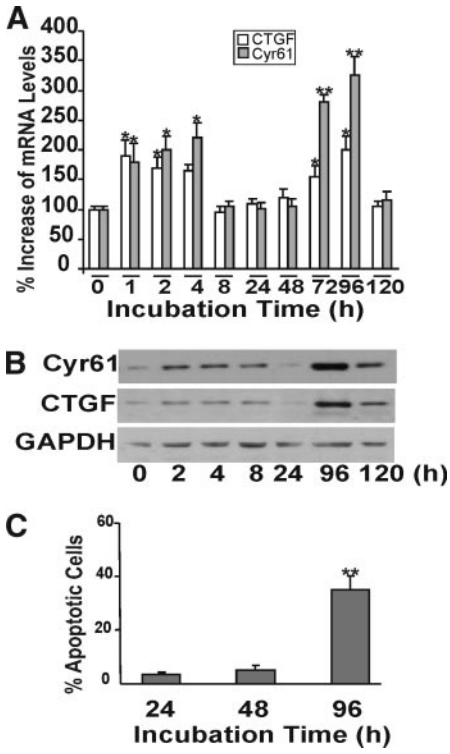

FIG. 1. AGE-BSA induces Cyr61 and CTGF gene expression and apoptosis of RRPs. Cultured pericytes were exposed to AGE-BSA (100 μg/ml) for up to 120 h. A, The Cyr61 and CTGF transcript levels were determined by real-time PCR using specifically designed primers overlapping two adjacent exons and normalized to 18S rRNA levels. Data are given as means ± SE of three separate experiments in which each time point was tested in quadruplicate. To facilitate comparisons among different experiments, the levels of either Cyr61 or CTGF mRNAs in the control were set to 100%. *, $P < 0.05$; and **, $P < 0.01$ *vs.* control cells. B, Cyr61 and CTGF proteins in RRPs exposed to AGE-BSA were detected in cellular lysates by Western immunblotting. To control for total protein loading, the same blots were probed with an anti-GAPDH antibody. Immunodetection was performed by enhanced chemiluminescence. C, Apoptotic cells were identified using the TUNEL assay. Representative histograms are shown for 24, 28, and 96 h after AGE-BSA treatment. Experiments have been repeated at least five times. Data are mean ± SE. **, $P < 0.01$ *vs.* the experimental points 24 and 48 h of incubation.

AGE-BSA for 4 and 96 h, respectively. These changes correlated well with those seen at the protein level (Fig. 1B). Cells treated with BSA alone did not result in Cyr61 and CTGF gene induction, suggesting specificity of AGE-BSA effects on retinal pericytes (data not shown).

AGE-BSA-induced pericyte death was determined using the TUNEL assay. Ninety-six-hour exposure to AGE-BSA significantly increased the number of TUNEL-positive cells (Fig. 1C). There was no significant increase in the number of apoptotic cells at earlier time points (*e.g.* 24 and 48 h). BSA treatment of the cells for 4 d resulted in less than 5% of cell death (data not shown). AGE-BSA-induced cell death was concomitant with the stronger elevation of Cyr61 and CTGF levels, suggesting a potential role of these proteins in the pro-apoptotic effects of AGE products.

Adenovirus-mediated expression of Cyr61 and/or CTGF induces apoptosis of retinal pericytes

We examined the specific effects of Cyr61 and CTGF proteins on retinal pericyte death by transducing the cells with replication-deficient adenoviruses overexpressing either the Ad-Cyr61 or Ad-CTGF genes. Cells infected with an empty adenoviral vector (Ad-V) were used as controls. A progressive increase of Cyr61 and CTGF proteins was detected by Western immunoblotting after the adenoviruses were added (Fig. 2A). Upon incubation in serum-free medium, cells overexpressing Cyr61 or CTGF underwent a dramatic change in cell morphology and adherence (data not shown). Cell death was, first, assessed using the TUNEL assay. As shown in Fig. 2B, TUNEL-positive nuclei were readily detected in cells infected with either Ad-Cyr61 or A-CTGF but not the control Ad-V. Statistical analyses of data indicate that 50 and 31% of cells underwent apoptosis upon expression of Cyr61 and CTGF, respectively (Fig. 2C, **, $P < 0.01$ *vs.* Ad-V). Overexpression of both Cyr61 and CTGF in RRPs had an additive effect suggesting that their coexpression amplified the death signal.

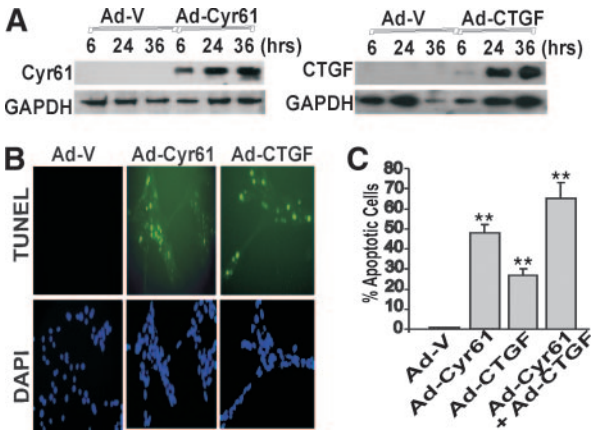

FIG. 2. Adenovirus-mediated expression of Cyr61 and/or CTGF induces apoptosis of RRPs. Cells were plated for 24 h in serum-containing medium with Ad-V, Ad-Cyr61, or Ad-CTGF. Cells were incubated in serum-free medium and processed for further analyses. A, Cell lysates were prepared and their protein content fractioned in a 10% SDS-polyacrylamide gel and analyzed for the expression of Cyr61 and CTGF proteins by Western blot/immunodetection assay. B, RRPs were fixed, permeabilized, and subjected to the TUNEL assay. Cells were counterstained with DAPI for nuclear localization. TUNEL-positive cells were detected with an FITC-conjugated antibody. C, Quantification of TUNEL-positive RRPs upon overexpression of the Cyr61 and/or CTGF genes. The percentage of cells scored for apoptosis was determined and represent mean ± SE (n = 4). **, $P < 0.01$ *vs.* Ad-V.

Apoptosis of RRPs is mediated by anoikis

For many anchorage-dependent cells, the adherence to the matrix is a necessary condition for survival. Disruption of cell-matrix interactions results in loss of prosurvival signals culminating in cell death referred to as anoikis. We used the CytoSelect anoikis assay to determine whether RRPs undergo anoikis either when they were exposed to AGE-BSA or upon overexpression of Cyr61 or CTGF. First, cells were treated with either BSA alone or AGE-BSA and collected (both floating and attached cells) after 4 d. The cells were then plated in anchorage-resistant Hema-coated and control plates. EthD-1 was added after 6 h and the fluorescence was measured. As shown in Fig. 3A, AGE-BSA significantly increased the amount of apoptotic cells plated in anchorage-resistant and control plates. BSA treatment alone resulted in 22% increase ($P < 0.05$) of cell death when cells were plated in anchorage-resistant plates *vs.* control plates. AGE-BSA-induced cell death was increased by 63% if the cells were incubated in anchorage-resistant plates *vs.* control plates ($P < 0.01$). These data clearly support the idea that AGE-BSA-induced cell death was, at least in part, mediated by altered cell-matrix interactions, *i.e.* anoikis.

In parallel experiments, cells were incubated with Ad-Cyr61, Ad-CTGF, or Ad-V. Twenty four hours later, cells were collected and tested for anoikis. Figure 3B shows that the amount of Ad-V-transduced cells able to survive and readhere to the tissue culture flasks significantly decreased when the cells were maintained in suspension in the anchorage-resistant *vs.* control plates, indicating that RRP adherence is critical for their survival. Overexpression of Cyr61 resulted in 74% increase of cell death in the anchorage-resistant plate and 59% increase in the control plate ($P < 0.05$). Differences between the control and Poly-Hema-coated plates may be due, at least in part, to the ability of the cells to produce their own matrix and readhere to it in the control plates. Similarly, overexpression of CTGF increased cell death in the anchorage-resistant (46%) *vs.* control plates (39%). Thus, both Cyr61 and CTGF induce anoikis-like cell death.

Effects of Cyr61 and CTGF on retinal pericyte adhesion

Cyr61 and CTGF have been shown to support adhesion of skin fibroblasts and endothelial cells but they induce deadhesion of mesangial cells (29, 30). Interestingly, one of the striking changes observed in retinal pericytes as they express increasing amounts of Cyr61 or CTGF proteins upon transduction with recombinant adenoviruses is their adoption of a rounded morphology and their detachment from the ECM. A large amount of cells appeared to either be completely detached or have less than five focal adhesion sites/cell (data not shown). Because anoikis is linked primarily to the loss of cell adhesion or the absence of cell adhesion-dependent signaling, we analyzed the effects of Cyr61 and CTGF as substrates on pericyte adhesion. As shown in Fig. 4A, a poor cell

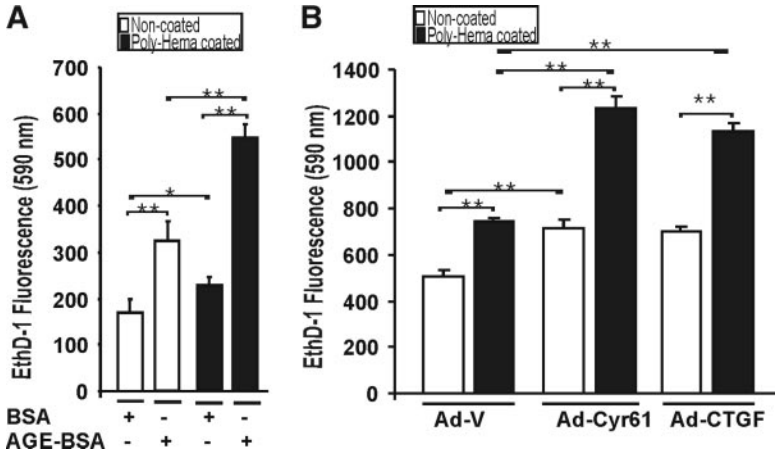

FIG. 3. Apoptosis of RRPs is mediated by anoikis. A, RRPs were incubated with either BSA or AGE-BSA (100 μg/ml) for up to 4 d. The cells were then collected and plated in anchorage-resistant ploy-Hema-coated and control non-coated plates. EthD-1 was added after 6 h, and the fluorescence due to the interaction of EthD-1 with damaged cell membranes was measured at 590 nm. B, Cells were incubated with Ad-V, Ad-Cyr61, or Ad-CTGF. Twenty-four hours after incubation with the adenoviruses, cells were collected and subjected to the anoikis assay as described in A. Values are the means ± SE (n = 3). **, $P < 0.01$.

adhesion occurs on BSA, whereas laminin, type IV collagen, or type I collagen dose-dependently increased cell adhesion. Maximal adhesion was supported on type IV collagen-coated wells, which is consistent with the notion that basement membrane proteins are the natural support for pericytes in retinal vessels. In contrast, coating concentrations of Cyr61 or CTGF ranging from 0.5 to 20 μg/ml resulted in a markedly decreased pericyte adhesion. Cyr61 and CTGF proteins supported well endothelial cell adhesion within the range of the concentrations used (data not shown), suggesting that direct cytotoxicity of these proteins did not cause deadhesion of pericytes. Similarly, Cyr61 and CTGF used as substrate decreased, in a dose-dependent manner, pericyte adhesion to type IV collagen-coated wells, which is consistent with the antiadhesive properties of Cyr61 and CTGF vis-à-vis pericytes (Fig. 4B).

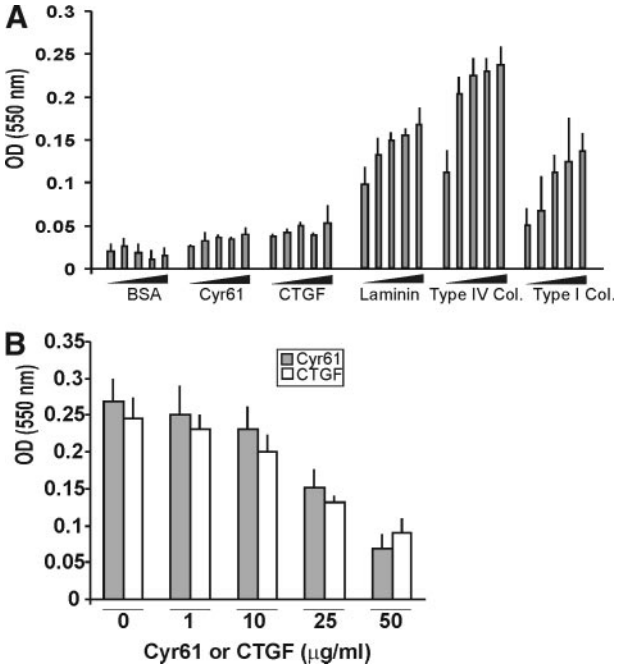

FIG. 4. Adhesion of RRPs to Cyr61 and CTGF. A, RRPs were plated in microtiter plates precoated with increasing concentrations of BSA (0.75, 1.25, 2.5, 5, 10 μg/ml); Cyr61 (1.5, 3, 6, 12, 24 μg/ml); CTGF (1.5, 3, 6, 12, 24 μg/ml); EHS laminin (1.5, 2.5, 5, 10, 20 μg/ml), type IV collagen (0.75, 1.25, 2.5, 5, 10 μg/ml); or type I collagen (0.75, 1.25, 2.5, 5, 10 μg/ml). After incubation at 37 C for 30 min, attached cells were fixed with paraformaldehyde and stained with crystal violet. The dye was solubilized with 2% SDS and quantified by absorbance at 550 nm. The data shown are the means ± SE of three determinations. The experiments were repeated twice with similar results. B, RRPs were plated in microtiter plates precoated with type IV collagen (1.50 μg/ml) and increasing concentrations of either Cyr61 (1, 10, 25, 50 μg/ml) or CTGF (1, 10, 25, 50 μg/ml). The data shown are the means ± SE of three determinations.

Cyr61 and CTGF alter anchorage-dependent signaling in retinal pericytes

The anchorage of cells to ECM proteins is mainly mediated by integrins, which undergo phosphorylation of their tyrosine and serine residues, glycosylation of their extracellular amino acid residues, and oligomerization/clustering. Clusters of integrins induce autophosphorylation and recruitment of cytoplasmic tyrosine kinase proteins to focal adhesion (FA) complexes composed essentially of focal adhesion kinase, paxillin, talin, and actin. As the cells release their ECM attachments, they reorganize their FA complexes, which disassemble and reconcentrate ventrally underneath the cells (31). In this process, FA structural proteins are dephosphorylated and their cell content diminishes. The early tyrosine dephosphorylation of FA kinase and the decreased amount of paxillin are sufficient to initiate cell death by anoikis (32, 33). Therefore, we examined whether pericyte treatment with AGE-BSA affects the tyrosine phosphorylation state of the proteins at focal adhesion points. As shown in Fig. 5A, phosphotyrosine staining revealed an intense punctate at the cell periphery in BSA-treated cells characteristic of phosphotyrosine proteins at focal adhesion points. However, phosphotyrosine staining was markedly reduced in AGE-BSA-treated cells, which appeared to have lost their elongated shape as well, a typical feature of cells undergoing apoptosis. A similar pattern for paxillin staining can be observed, suggesting a marked decrease of paxillin in AGE-BSA-treated cells (Fig. 5B).

We also examined whether these anoikis-associated events occur upon overexpression of either Cyr61 or CTGF in pericytes. Immunohistochemical analyses with antiphosphotyrosine and antipaxillin antibodies revealed typical arrowhead-shaped dots localized at the periphery of control cells at focal adhesion sites (Fig. 5, C and D, respectively). In

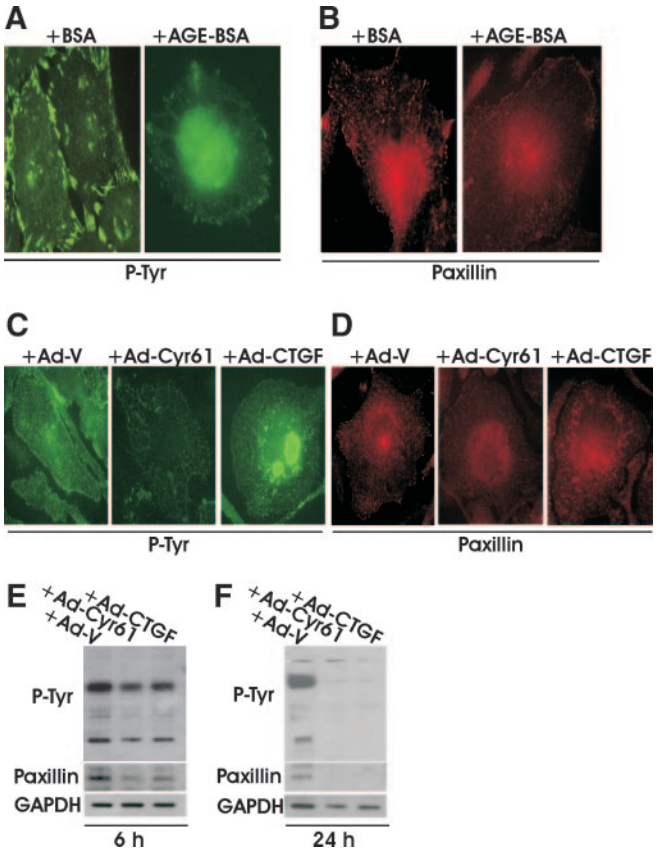

FIG. 5. Effects of AGE-BSA, Cyr61, and CTGF on anchorage-dependent signaling. A and B, RRPs were incubated with either BSA or AGE-BSA (100 μg/ml) for up to 4 d. Cells were fixed in paraformaldehyde solution and immunostained with either antiphosphotyrosine (P-Tyr; A) or antipaxillin antibody (B). The immunostaining was detected with FITC- and TRITC-conjugated IgG, respectively, and visualized by fluorescence microscopy. C and D, RRPs were incubated with Ad-V, Ad-Cyr61, or Ad-CTGF for 6 h; fixed in paraformaldehyde solution; and immunostained with either anti-P-Tyr (C) or antipaxillin (D) antibodies. E and F, Equal amounts of proteins (20 μg) from cells treated with Ad-V, Ad-Cyr61, or Ad-CTGF for 6 h (E) or 24 h (F) were fractioned by electrophoresis; transferred to a nitrocellulose membrane; and immunoblotted sequentially with anti-P-Tyr, antipaxillin, and anti-GAPDH antibodies. Signals were detected by chemiluminescence. The experiments have been repeated at least twice with nearly similar results.

contrast, phosphotyrosine protein and paxillin staining distinctly decreased in Cyr61-treated cells, which adopted a rounded morphology after an incubation time of 6 h, as the cells begin expressing increasing amounts of Cyr61. CTGF-treated cells also showed a reduced staining, although less intense than that of Cyr61-treated cells. Western blot analysis showed decreased phosphotyrosine protein and paxillin band intensities in Cyr61- and CTGF-treated cells after an incubation time of 6 h (Fig. 5E). The changes of protein band intensity were not as dramatic as those seen by immunostaining, suggesting that the immunohistochemical approach was more sensitive than Western blotting analysis of proteins. However, a longer incubation time period (24 h) resulted in cell detachment and drastic decreases of phosphotyrosine protein and paxillin band intensities (Fig. 5F).

We further examined actin cytoskeletal alterations using phalloidin staining. As shown in Fig. 6, control cells were elongated and contained an extensive network of stress fibers. In contrast, Cyr61- and CTGF-expressing cells exhibited mostly a peripheral membrane-associated ring of actin characteristic of apoptotic cells. However, these changes developed rapidly in Cyr6- expressing cells and relatively slowly in CTGF-expressing cells, which may account for the higher proapoptotic potential of Cyr61, compared with that of CTGF. Taken together, these observations suggest that Cyr61 and CTGF induce morphological and cytoskeletal alterations consistent with anoikis.

Cyr61 and CTGF induce dephosphorylation events in RRPs

Because the loss of matrix adhesion is a known inducer of cell death, the antiadhesive activity of Cyr61 and CTGF may be viewed as the mechanism for their proapoptotic activity. By decreasing phosphotyrosine protein levels at the cell surface, Cyr61 and CTGF clearly affect phosphorylation events in the cells. To further substantiate this hypothesis, cells were plated in microtiter plates coated with Cyr61 and/or type IV collagen in the presence and in the absence of either phosphatase or kinase inhibitors. The extent of cell adhesion was determined. As shown in Fig. 7A, both sodium orthovanadate (20 μM), a tyrosine phosphatase inhibitor, and okadaic acid (50 nM), a serine threonine phosphatase inhibitor, significantly increased cell adhesion in type IV collagen/Cyr61-coated wells. In contrast, genistein, a tyrosine kinase inhibitor, increased cell detachment on type IV collagen. Consistent with these data, incubation of the cells with either orthovanadate or okadaic acid decreased Cyr61-induced anoikis, whereas genistein further increased the levels of cell undergoing apoptosis as determined by the anoikis assay (Fig. 7B). Thus, by inhibiting dephosphorylation events, phosphatase inhibitors maintain the target of tyrosine and serine/threonine kinases in a phosphorylation/active state and prevent cell detachment and apoptosis.

Cyr61 and CTGF activate the intrinsic mitochondrial pathway of apoptosis in RRPs

To examine the apoptotic pathways associated with the proanoikis effects of Cyr61 and CTGF, we determined the levels Bax and Bcl2 as well as the effects of specific inhibitors of caspases on RRPs. Western blot and densitometric analyses showed that adenovirus-mediated expression of either Cyr61 or CTGF induced a 2-fold increase (Fig. 8A; **, $P < 0.05$ *vs.* Ad-V) of Bax protein levels, a proapoptotic molecule

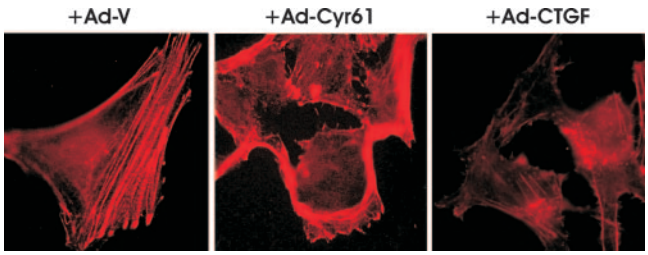

FIG. 6. Cyr61 and CTGF induce reorganization of cytoskeletal actin. RRPs transduced with Ad-V, Ad-Cyr61, or Ad-CTGF were fixed in paraformaldehyde solution, permeabilized with a detergent, and stained with TRITC-conjugated phalloidin.

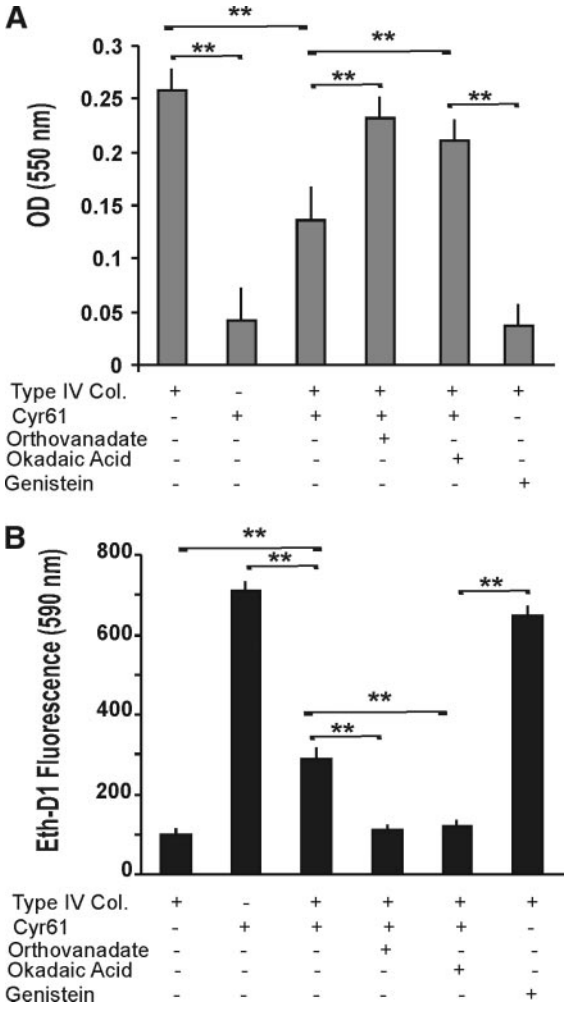

FIG. 7. Modulation of Cyr61 activity by phosphatase inhibitors. A, RRPs were pretreated with either sodium orthovanadate (20 μM), okadaic acid (50 nM), or genistein (100 μM) for 30 min and then plated in microtiter plates precoated with a mixture of type IV collagen (2.5 μg/ml) and Cyr61 (10 μg/ml). After 30 min incubation at 37 C, cell adhesion was quantified as described in Fig. 4. The data shown are the means ± SE of three separate experiments. **, $P < 0.05$. B, Cells were treated as described in A and incubated for up to 6 h. Cells were then tested for anoikis using the anoikis assay as described in *Materials and Methods*. The data shown are the means ± SE (n = 3). Data are representative of two separate experiments with similar results.

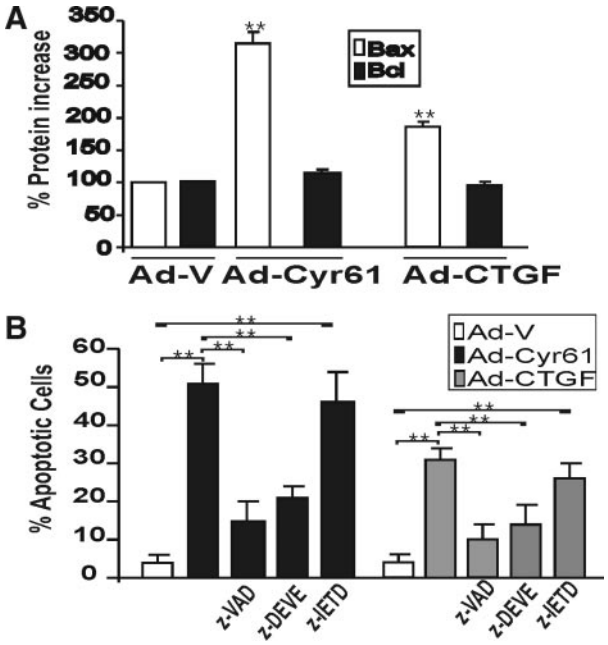

FIG. 8. Cyr61 and CTGF activate the intrinsic pathway of apoptosis. A, RRPs were transduced with Ad-V, Ad-Cyr61, or Ad-CTGF. The levels of Bax and Bcl2 proteins were determined by densitometric scanning of immunoblots from cell lysates. Each *bar* represents the means ± SE of three different isolates each of which was analyzed in duplicate. **, $P < 0.05$ *vs.* Ad-V lysate. B, RRPs infected with Ad-V, Ad-Cyr61, or Ad-CTGF were incubated with each of the following caspase inhibitors: Z-VAD (50 μM), Z-DEVD (50 μM), and Z-IETD (100 μM) for up to 24 h. Apoptotic cells were identified by TUNEL assay and their percentage was determined. Each *bar* represents the means ± SE of three experiments. **, $P < 0.01$.

known to oligomerize and localize to the outer mitochondrial membrane to facilitate cytochrome c release in apoptotic cells. Surprisingly, the expression of the antiapoptotic factor Bcl-2 was not significantly changed. It is noteworthy that the sole increase of Bax levels expression alters the Bax to Bcl ratio, which is often sufficient to increase the cell's susceptibility to apoptosis.

To determine whether and which caspases are involved in Cyr61- and CTGF-induced apoptosis, RRPs infected with Ad-V, Ad-Cyr61, or Ad-CTGF were incubated with cell permeable, irreversible inhibitors of either all caspases (z-VAD-fmk), caspase-3 (z-DEVD-fmk), or caspase-8 (z-IETD-fmk) for up to 24 h. Apoptotic cell death was assessed by TUNEL assay. As shown in Fig. 8B, inhibition of either all caspases or caspase-3 significantly reduced the number of apoptotic pericytes overexpressing Cyr61 or CTGF, whereas inhibition of caspase-8 had no significant effects.

Identification of Cyr61 target genes using apoptosis-specific arrays

We screened an apoptosis-specific array to identify the pro- and antiapoptotic genes targeted by the Cyr61 and CTGF proteins. For this purpose, RRPs were infected with either Ad-GFP or Ad-Cyr61 adenoviral vectors and incubated in serum-free medium for 24 h. Total RNA was isolated and converted into biotin-labeled cRNA. The labeled RNA was then used for hybridization to Rat GEArrays membranes on which 113 oligonucleotides representing pro- and antiapoptotic genes have been printed. Hybridization signals were detected by chemiluminescence. Negative control oligonucleotides printed on the arrays (*e.g.* blank spots, pUC 18, artificial sequences) yielded no signal (Fig. 9A). Approximately 43% of the oligonucleotides printed on the arrays hybridized to cRNA probes among which 21 genes were found to be differentially expressed using a 2-fold cutoff. These include Akt1, Bax, Bad, Bid, caspase-3, caspase-6, Check 1, Check 2, and GADD45a. Differential expression of several genes was further tested by using real-time PCR. As shown in Fig. 9B, the expression of the proapoptotic factors p53, Bax, Bad, and GADD45a was significantly up-regulated, whereas that of antiapoptotic factors such as Api2/Birc2 and atf-5 was down-regulated by either Cyr61 or CTGF. Inter-

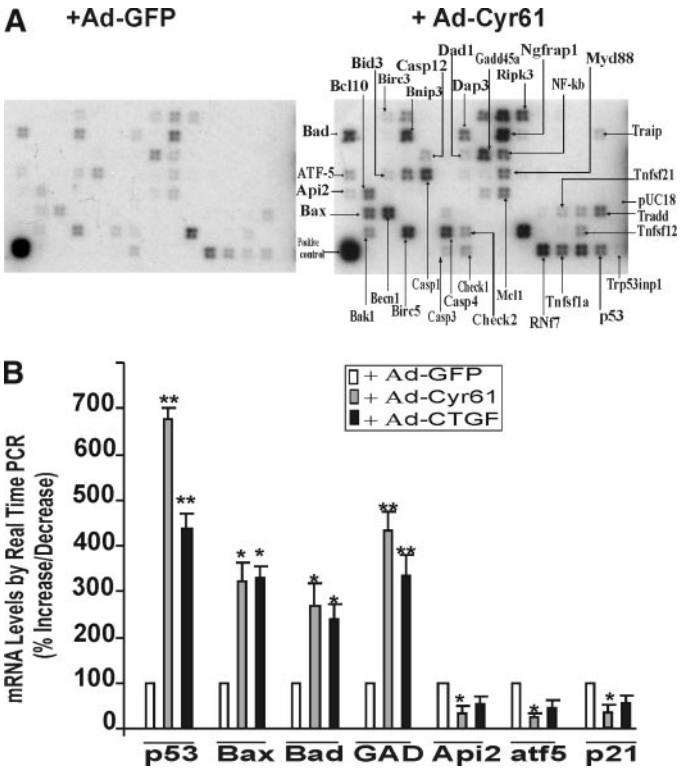

FIG. 9. Identification of Cyr61 target genes using pathway-specific GEArray profiling. A, Total RNA (2 μg) from Ad-GFP- and Ad-Cyr61-infected RRPs was converted to biotin-labeled cRNA using the TrueLabeling-AMP amplification system as described in *Materials and Methods*. The cRNAs were hybridized to separate rat apoptosis Oligo GEArray membranes on which 113 pro- and antiapoptotic genes have been spotted. The hybridization signals were detected by chemiluminescence. B, The mRNA levels of selected Cyr61 target genes, p53, Bax, BAD, GAD/GADD45a, Api2, atf-5, and p21^{WAF1} were quantified by real-time PCR and normalized to the 18S rRNA levels. Data are given as means ± SE, n = 3. ** $P < 0.01$; *, $P < 0.05$ *vs.* the control Ad-GFP.

estingly, several of the Cyr61 target genes such as akt1, Bad, Bax, Bid, caspase-3, caspase-6, and GADD45a have been functionally grouped as p53- and DNA damage-induced apoptosis genes (34). Indeed, several members of the Bcl family such as Bax, Bad, and Bid are known to be under the transcriptional control of p53. These proteins constitute a critical intracellular checkpoint of apoptosis. Meanwhile, in addition to the genes imprinted on the GEArray, we found that the overexpression of Cyr61 or CTGF reduced the transcript levels of the small GTPase, p21^{WAF1}, which is also a p53 target gene. On another hand, the differential expression of other p53 gene targets such as AIP-1, Fas, Prdx2, Bnip3, and Rnf7 could not be confirmed by real-time PCR (data not shown), which underscores limitations of the GEArray approach. Taken together, these data suggest that the p53-mediated anoikis pathway plays an important role in Cyr61- and CTGF-induced retinal pericyte apoptosis.

Cyr61- and CTGF-induced MMP-2 gene expression mediates, at least in part, RRP apoptosis

Expression of either Cyr61 or CTGF has been previously associated with changes of gene programs for cell proliferation, ECM synthesis, and angiogenesis (35, 36). Therefore, we determined the mRNA levels of several putative Cyr61 and CTGF target genes including VEGF-A, type IV collagen, laminins, and MMP-2, -3, and -9 in cells expressing Cyr61 and CTGF. We found that either Cyr61 or CTGF induced a 2- to 3-fold increase in the mRNA levels for MMP-2, compared with control (Fig. 10). The mRNA levels of VEGF-A was significantly increased in Cyr61- but not CTGF-overexpressing cells. Conversely, neither Cyr61 nor CTGF affected the expression profile of α1(IV) collagen, β1-laminin, MMP-3, and MMP-9. In-gel gelatin zymography revealed a single MMP-2 band corresponding to the activated form of MMP-2 in conditioned medium from Cyr61- and CTGF-overexpressing cells (Fig. 11A). Neither the active nor latent forms of MMP-2 were detected in GFP-overexpressing cells. Thus, the MMP-2 gene, which has been shown to be under the control of p53 (37), is a Cyr61 and CTGF target gene as well.

Increased perivascular localization of MMP-2 has previously been observed in the retinal capillaries at the early stages of diabetes and has appeared to occur concomitantly with increased Cyr61 and CTGF gene expression, suggesting a cause-and-effect relationship (17, 38). To determine whether MMP-2 expression and activation mediate the proapoptotic effects of Cyr61 and/or CTGF on pericytes, RRPs infected with Ad-V, Ad-Cyr61, or Ad-CTGF were incubated with SB3CT, a specific inhibitor of MMP-2, and cell death was assessed using the TUNEL assay. As shown in Fig. 11B, the number of apoptotic cells was significantly reduced but not completely abolished in the presence of the MMP-2 inhibitor, SB3CT in cells overexpressing either Cyr61 or CTGF. Consistent with this result, incubation of RRPs with purified active MMP-2 significantly increased the number of apoptotic cells (+19%) (Fig. 11C). Taken together, these results suggest that the apoptogenic activity of the Cyr61 and CTGF proteins is partly mediated by MMP-2.

Discussion

Anoikis, a form of cell death triggered by inappropriate or inadequate contacts between the cells and the ECM, regu-

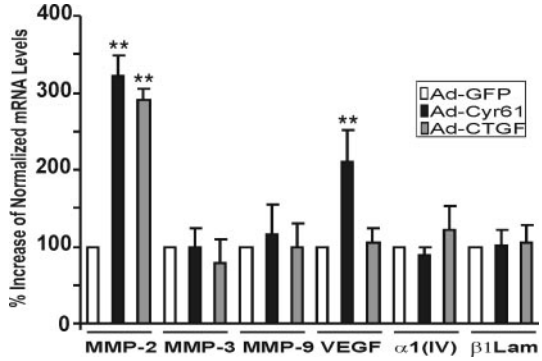

FIG. 10. Expression profile of putative Cyr61 and CTGF target genes in RRPs. RRPs were transduced with Ad-GFP, Ad-Cyr61, or Ad-CTGF and incubated in serum-free medium for 24 h. Genomic DNA-free RNA was prepared and reverse transcribed. The mRNA levels of MMP-2, -3, and -9, VEGF-A, α1(IV) collagen and β1-laminin chain were determined using real-time PCR and normalized to the 18S rRNA levels. Data are given as means ± SE, n = 4. **, $P < 0.05$ *vs.* Ad-GFP control.

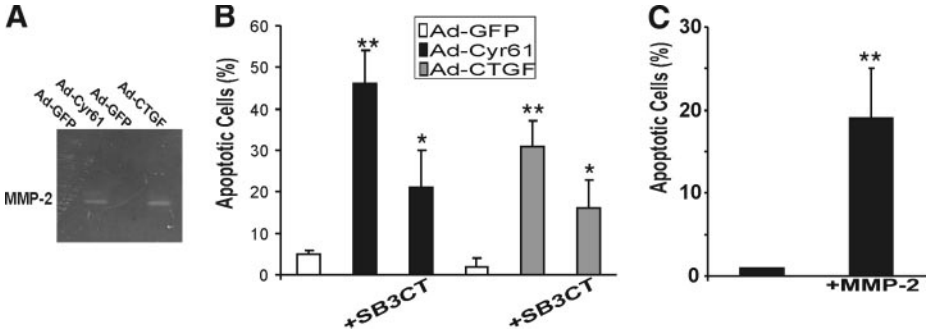

FIG. 11. Cyr61- and CTGF-induced MMP-2 gene expression mediates RRP apoptosis. A, In-gel zymography of conditioned medium from Ad-GFP-, Ad-Cyr61-, and Ad-CTGF-transduced cells. B, Inhibition of MMP-2 reduced Cyr61- and CTGF-induced apoptosis. RRPs expressing Ad-GFP, Ad-Cyr61, or Ad-CTGF were incubated with SB3CT (1 nM) for 24 h in serum-free medium. The percentage of apoptotic cells was determined using TUNEL assay. **, $P < 0.05$ *vs.* Ad-GFP; *, $P < 0.05$ *vs.* Ad-Cyr61 or Ad-CTGF, (n = 4). C, Cultured RRPs were treated with active MMP-2 (1 nM) for up to 16 h. Apoptotic cells were identified by TUNEL assay and counted. **, $P < 0.05$ *vs.* Ad-GFP (n = 3).

lates both physiological (*e.g.* tissue homeostasis and turnover) and pathological processes (*e.g.* tissue degeneration and tumorigenesis). Anoikis was initially observed for endothelial and epithelial cells for which attachment to the ECM, even in the presence of serum, is required to prevent cell death. However, initiation of anoikis is still a debatable issue as the initiating factors that bring about cell detachment from their substrate and propel the cells in the apoptotic pathway are not well understood. Our data showed that the Cyr61 and/or CTGF proteins promote detachment and anoikis of retinal pericytes. When used as substrates for cell attachment and compared with the constitutively expressed ECM proteins such as type IV collagen and laminin, both Cyr61 and CTGF exhibited antiadhesive and apoptogenic activities vis-à-vis retinal pericytes. Clearly, dynamic changes of the ECM composition, and thus cell-matrix interactions, are conducive to compromising pericyte survival.

As matricellular proteins, Cyr61 and CTGF do not assume a direct structural role in the matrix but modulate cell function and cell-matrix interactions. Other matricellular proteins such as thrombospondin, tenascin-C, and secreted protein acidic and rich in cysteine have been found to negatively regulate cell adhesion as well and reduce it to, at least, a state of intermediate cell adhesion (39). The type I repeat of thrombospondin 1, which is found in thrombospondin, Cyr61, and CTGF, has been shown to specifically induce endothelial cell deadhesion and apoptosis/anoikis, although adhesive properties have been assigned to this domain in hepatic stellate cells (40, 41). The antiadhesion properties of thrombospondin entail disassembly of focal adhesion characterized by unbundling of actin stress fibers and depletion of several focal adhesion proteins. Cyr61 and CTGF act, seemingly, along a similar pathway and their antiadhesive activity provides a mechanism for pericyte detachment and death. In Cyr61-treated cells, cytoskeletal actin rearranges into a peripheral ring in preparation of blebbing, which is characteristic of cells during the execution phase of apoptosis. The cytoskeletal changes develop rapidly in Cyr61-expressing cells and relatively slowly in CTGF-expressing cells, which may account for the higher proapoptotic potential of Cyr61. During this process, the link between the actin cytoskeleton and the plasma membrane may be broken focally allowing blebs to protrude at sites in which the plasma membrane is no longer attached to the cytoskeleton (42). However, membrane blebbing is cell type and stimulus dependent (42, 43). Whether both Cyr61 and CTGF induce membrane blebbing is unknown and will be investigated in future studies.

Interestingly, our data are at variance with a previous report showing that Cyr61 and CTGF trigger death of rat-1 fibroblasts through their cell adhesive function mediated by $\alpha_6\beta_1$ integrin (44). Cyr61 and CTGF have been shown to recognize various integrin receptors, although such interactions are complex and vary as a function of the type of integrins, the domain location in these proteins, and the cell type (45). Paradoxically, Cyr61-$\alpha_6\beta_1$ integrin interactions promote spreading/survival of skin fibroblasts and activate a gene program for angiogenesis (29, 46). Complicating further the matter is the observation that Cyr61 and CTGF promote cell migration/motility as well, which implies that they also exhibit anti-adhesive effects to allow efficient cell migration (47, 48). Whereas these observations are intriguing in their own right because cell adhesion presumably advocates cell survival instead of cell migration or death, they underscore the complex mechanisms of matricellular activities. Namely, the matricellular concept of these proteins may account for their puzzling features and the apparently contradictory properties reported in different studies. The activities of matricellular proteins are, indeed, cell type dependent and contextual in that they depend on the availability of receptors/binding partners and the ECM composition, which varies for each cell type. Anchorage-dependent cells such as cultured pericytes produce their own ECM to which they adhere (49). A potential explanation for the antiadhesive activities of Cyr61 and CTGF vis-à-vis pericytes is that as substrates, these proteins compete with the constitutively expressed ECM proteins for integrin binding. The excessive accumulation of these protein in the ECM may initiate deadhesion between pericytes and their surrounding ECM protein substrate, by converting strong cell-ECM interactions into weak ones. Under these conditions, the intracellular signaling pathways (*e.g.* tyrosine kinase phosphorylation cascades) that are normally triggered by contact between integrins and the constitutively expressed ECM proteins may either be turned off or replaced by others.

Two types of data support these observations. First, the changes of cell shape and morphology of pericytes indicate

that Cyr61 and CTGF provoke cell detachment possibly by inducing integrin disengagement. It is now well appreciated that integrin engagement or disengagement regulates cell proliferation and survival (50). In osteoblasts, unoccupied $\alpha_v\beta_3$-integrin induces apoptosis by transmitting a positive death signal, whereas in epithelial cells, the integrin β4 subunit can be cleaved by caspases, which disrupts hemidesmosome assembly and induces cell death (51, 52). There is, however, also clear evidence that integrin signaling alone is not sufficient to prevent anoikis (53). Second, the antiadhesive activity of Cyr61 and CTGF was associated with dephosphorylation events. Antagonizing the activity of phosphatases by sodium orthovanadate or okadaic acid maintained the targets of tyrosine kinases in a phosphorylation state and reduced pericyte deadhesion and death. However, these Cyr61-associated dephosphorylation events are cell type specific because in human primary fibroblasts, immobilized Cyr61 activates focal adhesion kinase and paxillin (54). Therefore, conflicting cell type-specific signals arise from Cyr61-cell interactions, and further work is needed to define the integration and regulation of the subsequent responses.

Meanwhile, our data showed that both Cyr61 and CTGF up-regulated the expression of the MMP-2 gene and increased MMP-2 activity, which mediates, at least in part, pericyte apoptosis. Morphological manifestations of cells undergoing anoikis can be seen in recombinant MMP-2-treated cells (data not shown). Thus, the process of Cyr61- and CTGF-induced anoikis embraces, perhaps, the dissolution by MMP-2 of interactions through pericellular proteolysis of molecules involved in cell-matrix and cell-cell interactions. In fact, there are several potential mechanisms for the apoptogenic activity of MMP-2. First, the collagenolytic activity of MMP-2 may induce pericyte death via degradation and removal of survival signals emanating from the ECM proteins. Type IV collagen, the major structural element of the basement membranes in which pericytes are embedded in retinal capillaries, is the prime target of MMP-2 activity. Second, MMP-2 may, in part, induce ECM degradation and release of modular breakdown products with a potent proapoptotic activity. In particular, proteolytic fragments of type IV collagen (*e.g.* tumstatin) and type XVII collagen (*e.g.* endostatin) have been shown to induce apoptosis of endothelial cells (55). Third, the proper proapoptotic activity of MMP-2 may compromise survival of anchorage-dependent cells like retinal pericytes. In ventricular myocytes, MMP-2 mediates β-adrenergic receptor-stimulated apoptosis via both direct interaction with β1-integrins and poly-ADP-ribose-polymerase cleavage (56). Further studies are needed to elucidate the mechanism of MMP-2-mediated apoptosis of retinal pericytes.

Another interesting finding of this study is the identification of the proapoptotic genes activated by Cyr61. These include Bad, Bax, Casp3, Casp6, Check1, Check2 Gadd45a, p53, and Trp53inp1. Most of these genes have been functionally grouped as p53 target genes. The MMP-2 gene has also been shown to be transcriptionally activated by p53, suggesting an important role of p53 as a mediator of Cyr61 and CTGF activity in pericytes (37). The p53 protein is known as both a downstream target of Cyr61 in cancer cells and a critical regulatory factor of program cell death during anoikis (34, 57). In particular, studies have shown that anoikis can be suppressed by transfection of fibroblasts with a dominant-negative form of p53 (43). Survival signals mediated by the a_6b_4 integrin can be effective only in p53-defective cells (58). Mechanistically, p53 was shown to target the protein called phosphatase and tensin homolog or phosphatase and tensin homolog (PTEN), which dephosphorylates focal adhesion kinase and phosphatidyl inositol 3,4,5 triphosphate, thereby antagonizing their function in cell survival (59). The p53-PTEN interregulation provides a plausible link between p53 activation and suppression of integrin-mediated survival signaling because PTEN was shown to restore anchorage dependency in anoikis-resistant cells (43).

Functionally, accumulation of Cyr61 and/or CTGF in normal retinal capillaries is likely to compromise retinal capillary integrity and precipitate their closure and degeneration, an important vascular feature of background diabetic retinopathy. *In vivo* studies have shown that both Cyr61 and CTGF are downstream effectors of AGE products in the diabetic retina and that mice treated with AGE products significantly up-regulated the expression of the Cyr61 and CTGF genes (17). Deleterious effects of AGE in diabetic mice can be prevented by injection of aminoguanidine, which down-regulates the expression of the Cyr61 and CTGF genes. In line with these observations, AGE-BSA-induced Cyr61 and CTGF gene expression in pericytes was markedly decreased in the presence of phosphatase inhibitors, which reversed, at least in part, the proapoptotic effects of Cyr61 and CTGF (data not shown). Thus, the accumulation of these matricellular proteins in the retinal capillaries at the onset of diabetes may alter the retinal capillary structure and organization. Studies have shown that impaired angiogenesis and reduced capillarization of skeletal muscles was associated with increased Cyr61 and CTGF levels in diabetic skeletal muscle (60). In addition, these matricellular proteins are susceptible to proteolytic degradation, which yields peptide fragments with, perhaps, biological activities of their own. A recent study showed that an N-terminal peptide derived from the CTGF protein accumulates in the vitreous of patients with active proliferative diabetic retinopathy (61). Therefore, Cyr61, CTGF, and/or their individual domains provide potential targets in therapeutic and biotechnological contexts.

Acknowledgments

The authors thank Dr. Julie Rushbrook for her critical discussion and review of this work. Our thanks go to S. Jatzke for technical help with the preparation of recombinant Cyr61.

Received October 16, 2007. Accepted December 31, 2007.

Address all correspondence and requests for reprints to: Dr. Brahim Chaqour, Department of Anatomy and Cell Biology, State University of New York Downstate Medical Center, Brooklyn, New York 11203. E-mail: bchaqour@downstate.edu.

This work was supported by grants from the Juvenile Diabetes Research Foundation (to B.C.) and the Deutsche Forschungsgemeinschaft (to N.S.).

Disclosure statement: H.L., R.Y., A.C., N.S., and B.C. have nothing to declare. B.T. is employed by QBM Cell Science.

References

1. **Chen Y, Du XY** 2007 Functional properties and intracellular signaling of CCN1/Cyr61. J Cell Biochem 100:1337–1345
2. **Perbal B** 2004 CCN proteins: multifunctional signalling regulators. Lancet 363:62–64
3. **Chaqour B, Goppelt-Struebe M** 2006 Mechanical regulation of the Cyr61/CCN1 and CTGF/CCN2 proteins. FEBS J 273:3639–3649
4. **Chaqour B, Yang R, Sha Q** 2006 Mechanical stretch modulates the promoter activity of the profibrotic factor CCN2 through increased actin polymerization and NF-κB activation. J Biol Chem 281:20608–20622
5. **O'Leary JM, Hamilton JM, Deane CM, Valeyev NV, Sandell LJ, Downing AK** 2004 Solution structure and dynamics of a prototypical chordin-like cysteine-rich repeat (von Willebrand factor type C module) from collagen IIA. J Biol Chem 279:53857–53866
6. **Chen CC, Young JL, Monzon RI, Chen N, Todorovic V, Lau LF** 2007 Cytotoxicity of TNFα is regulated by integrin-mediated matrix signaling. EMBO J 26:1257–1267
7. **Gao R, Brigstock DR** 2003 Low density lipoprotein receptor-related protein (LRP) is a heparin-dependent adhesion receptor for connective tissue growth factor (CTGF) in rat activated hepatic stellate cells. Hepatol Res 27:214–220
8. **Leask A, Abraham DJ** 2006 All in the CCN family: essential matricellular signaling modulators emerge from the bunker. J Cell Sci 119:4803–4810
9. **Leu SJ, Lam SC, Lau LF** 2002 Pro-angiogenic activities of CYR61 (CCN1) mediated through integrins αvβ3 and α6β1 in human umbilical vein endothelial cells. J Biol Chem 277:46248–46255
10. **Leu SJ, Liu Y, Chen N, Chen CC, Lam SC, Lau LF** 2003 Identification of a novel integrin α6β1 binding site in the angiogenic inducer CCN1 (CYR61). J Biol Chem 278:33801–33808
11. **Schober JM, Chen N, Grzeszkiewicz TM, Jovanovic I, Emeson EE, Ugarova TP, Ye RD, Lau LF, Lam SC** 2002 Identification of integrin α(M)β(2) as an adhesion receptor on peripheral blood monocytes for Cyr61 (CCN1) and connective tissue growth factor (CCN2): immediate-early gene products expressed in atherosclerotic lesions. Blood 99:4457–4465
12. **Segarini PR, Nesbitt JE, Li D, Hays LG, Yates III JR, Carmichael DF** 2001 The low density lipoprotein receptor-related protein/α2-macroglobulin receptor is a receptor for connective tissue growth factor. J Biol Chem 276:40659–40667
13. **Rachfal AW, Brigstock DR** 2005 Structural and functional properties of CCN proteins. Vitam Horm 70:69–103
14. **Brigstock DR** 2003 The CCN family: a new stimulus package. J Endocrinol 178:169–175
15. **Wilkinson-Berka JL, Fletcher EL** 2004 Angiotensin and bradykinin: targets for the treatment of vascular and neuro-glial pathology in diabetic retinopathy. Curr Pharm Des 10:3313–3330
16. **Kuiper EJ, Witmer AN, Klaassen I, Oliver N, Goldschmeding R, Schlingemann RO** 2004 Differential expression of connective tissue growth factor in microglia and pericytes in the human diabetic retina. Br J Ophthalmol 88:1082–1087
17. **Hughes JM, Kuiper EJ, Klaassen I, Canning P, Stitt AW, Van Bezu J, Schalkwijk CG, Van Noorden CJ, Schlingemann RO** 2007 Advanced glycation end products cause increased CCN family and extracellular matrix gene expression in the diabetic rodent retina. Diabetologia 50:1089–1098
18. **He Z, Way KJ, Arikawa E, Chou E, Opland DM, Clermont A, Isshiki K, Ma RC, Scott JA, Schoen FJ, Feener EP, King GL** 2005 Differential regulation of angiotensin II-induced expression of connective tissue growth factor by protein kinase C isoforms in the myocardium. J Biol Chem 280:15719–15726
19. **Twigg SM, Chen MM, Joly AH, Chakrapani SD, Tsubaki J, Kim HS, Oh Y, Rosenfeld RG** 2001 Advanced glycosylation end products up-regulate connective tissue growth factor (insulin-like growth factor-binding protein-related protein 2) in human fibroblasts: a potential mechanism for expansion of extracellular matrix in diabetes mellitus. Endocrinology 142:1760–1769
20. **Lantz M, Vondrichova T, Parikh H, Frenander C, Ridderstrale M, Asman P, Aberg M, Groop L, Hallengren B** 2005 Overexpression of immediate early genes in active Graves' ophthalmopathy. J Clin Endocrinol Metab 90:4784–4791
21. **Zhou G, Li C, Cai L** 2004 Advanced glycation end-products induce connective tissue growth factor-mediated renal fibrosis predominantly through transforming growth factor β-independent pathway. Am J Pathol 165:2033–2043
22. **Podesta F, Romeo G, Liu WH, Krajewski S, Reed JC, Gerhardinger C, Lorenzi M** 2000 Bax is increased in the retina of diabetic subjects and is associated with pericyte apoptosis *in vivo* and *in vitro*. Am J Pathol 156:1025–1032
23. **Sakagami K, Wu DM, Puro DG** 1999 Physiology of rat retinal pericytes: modulation of ion channel activity by serum-derived molecules. J Physiol 521(Pt 3):637–650
24. **Stitt AW, Hughes SJ, Canning P, Lynch O, Cox O, Frizzell N, Thorpe SR, Cotter TG, Curtis TM, Gardiner TA** 2004 Substrates modified by advanced glycation end-products cause dysfunction and death in retinal pericytes by reducing survival signals mediated by platelet-derived growth factor. Diabetologia 47:1735–1746
25. **Beltramo E, Buttiglieri S, Pomero F, Allione A, D'Alu F, Ponte E, Porta M** 2003 A study of capillary pericyte viability on extracellular matrix produced by endothelial cells in high glucose. Diabetologia 46:409–415
26. **Brownlee M** 1992 Glycation products and the pathogenesis of diabetic complications. Diabetes Care 15:1835–1843
27. **Suzuma K, Naruse K, Suzuma I, Takahara N, Ueki K, Aiello LP, King GL** 2000 Vascular endothelial growth factor induces expression of connective tissue growth factor via KDR, Flt1, and phosphatidylinositol 3-kinase-akt-dependent pathways in retinal vascular cells. J Biol Chem 275:40725–40731
28. **Schutze N, Kunzi-Rapp K, Wagemanns R, Noth U, Jatzke S, Jakob F** 2005 Expression, purification, and functional testing of recombinant CYR61/CCN1. Protein Expr Purif 42:219–225
29. **Chen N, Chen CC, Lau LF** 2000 Adhesion of human skin fibroblasts to Cyr61 is mediated through integrin α6β1 and cell surface heparan sulfate proteoglycans. J Biol Chem 275:24953–24961
30. **Crean JK, Furlong F, Mitchell D, McArdle E, Godson C, Martin F** 2006 Connective tissue growth factor/CCN2 stimulates actin disassembly through Akt/protein kinase B-mediated phosphorylation and cytoplasmic translocation of p27(Kip-1). FASEB J 20:1712–1714
31. **Bannerman DD, Sathyamoorthy M, Goldblum SE** 1998 Bacterial lipopolysaccharide disrupts endothelial monolayer integrity and survival signaling events through caspase cleavage of adherens junction proteins. J Biol Chem 273:35371–35380
32. **Gilmore AP** 2005 Anoikis. Cell Death Differ 12(Suppl 2):1473–1477
33. **van de WB, Nagelkerke JF, Stevens JL** 1999 Dephosphorylation of focal adhesion kinase (FAK) and loss of focal contacts precede caspase-mediated cleavage of FAK during apoptosis in renal epithelial cells. J Biol Chem 274:13328–13337
34. **Michalak E, Villunger A, Erlacher M, Strasser A** 2005 Death squads enlisted by the tumour suppressor p53. Biochem Biophys Res Commun 331:786–798
35. **Chen CC, Mo FE, Lau LF** 2001 The angiogenic factor Cyr61 activates a genetic program for wound healing in human skin fibroblasts. J Biol Chem 276:47329–47337
36. **Zhou D, Herrick DJ, Rosenbloom J, Chaqour B** 2005 Cyr61 mediates the expression of VEGF, αv-integrin, and α-actin genes through cytoskeletally based mechanotransduction mechanisms in bladder smooth muscle cells. J Appl Physiol 98:2344–2354
37. **Bian J, Sun Y** 1997 Transcriptional activation by p53 of the human type IV collagenase (gelatinase A or matrix metalloproteinase 2) promoter. Mol Cell Biol 17:6330–6338
38. **Yang R, Liu H, Williams I, Chaqour B** 2007 Matrix metalloproteinase-2 expression and apoptogenic activity in retinal pericytes: implications in diabetic retinopathy. Ann NY Acad Sci 1103:196–201
39. **Murphy-Ullrich JE** 2001 The de-adhesive activity of matricellular proteins: is intermediate cell adhesion an adaptive state? J Clin Invest 107:785–790
40. **Guo N, Krutzsch HC, Inman JK, Roberts DD** 1997 Thrombospondin 1 and type I repeat peptides of thrombospondin 1 specifically induce apoptosis of endothelial cells. Cancer Res 57:1735–1742
41. **Tong ZY, Brigstock DR** 2006 Intrinsic biological activity of the thrombospondin structural homology repeat in connective tissue growth factor. J Endocrinol 188:R1–R8
42. **Frisch SM, Screaton RA** 2001 Anoikis mechanisms. Curr Opin Cell Biol 13:555–562
43. **Grossmann J** 2002 Molecular mechanisms of "detachment-induced apoptosis—anoikis." Apoptosis 7:247–260
44. **Todorovicc V, Chen CC, Hay N, Lau LF** 2005 The matrix protein CCN1 (CYR61) induces apoptosis in fibroblasts. J Cell Biol 171:559–568
45. **Lau LF, Lam SC** 1999 The CCN family of angiogenic regulators: the integrin connection. Exp Cell Res 248:44–57
46. **Chen Y, Abraham DJ, Shi-Wen X, Pearson JD, Black CM, Lyons KM, Leask A** 2004 CCN2 (connective tissue growth factor) promotes fibroblast adhesion to fibronectin. Mol Biol Cell 15:5635–5646
47. **Gao R, Brigstock DR** 2006 A novel integrin α5β1 binding domain in module 4 of connective tissue growth factor (CCN2/CTGF) promotes adhesion and migration of activated pancreatic stellate cells. Gut 55:856–862
48. **Grzeszkiewicz TM, Kirschling DJ, Chen N, Lau LF** 2001 CYR61 stimulates human skin fibroblast migration through Integrin αvβ5 and enhances mitogenesis through integrin αvβ3, independent of its carboxyl-terminal domain. J Biol Chem 276:21943–21950
49. **Canfield AE, Allen TD, Grant ME, Schor SL, Schor AM** 1990 Modulation of extracellular matrix biosynthesis by bovine retinal pericytes *in vitro*: effects of the substratum and cell density. J Cell Sci 96(Pt 1):159–169
50. **Stupack DG, Cheresh DA** 2003 Apoptotic cues from the extracellular matrix: regulators of angiogenesis. Oncogene 22:9022–9029
51. **Werner ME, Chen F, Moyano JV, Yehiely F, Jones JC, Cryns VL** 2007 Caspase proteolysis of the integrin β4 subunit disrupts hemidesmosome assembly, promotes apoptosis, and inhibits cell migration. J Biol Chem 282:5560–5569
52. **Zhao H, Ross FP, Teitelbaum SL** 2005 Unoccupied α(v)β3 integrin regulates osteoclast apoptosis by transmitting a positive death signal. Mol Endocrinol 19:771–780
53. **Chen CS, Mrksich M, Huang S, Whitesides GM, Ingber DE** 1997 Geometric control of cell life and death. Science 276:1425–1428
54. **Chen CC, Chen N, Lau LF** 2001 The angiogenic factors Cyr61 and connective

tissue growth factor induce adhesive signaling in primary human skin fibroblasts. J Biol Chem 276:10443–10452
55. **Sudhakar A, Sugimoto H, Yang C, Lively J, Zeisberg M, Kalluri R** 2003 Human tumstatin and human endostatin exhibit distinct antiangiogenic activities mediated by $\alpha v\beta 3$ and $\alpha 5\beta 1$ integrins. Proc Natl Acad Sci USA 100: 4766–4771
56. **Menon B, Singh M, Ross RS, Johnson JN, Singh K** 2006 β-Adrenergic receptor-stimulated apoptosis in adult cardiac myocytes involves MMP-2-mediated disruption of $\beta 1$ integrin signaling and mitochondrial pathway. Am J Physiol Cell Physiol 290:C254–C261
57. **Tong X, Xie D, O'Kelly J, Miller CW, Muller-Tidow C, Koeffler HP** 2001 Cyr61, a member of CCN family, is a tumor suppressor in non-small cell lung cancer. J Biol Chem 276:47709–47714
58. **Bachelder RE, Ribick MJ, Marchetti A, Falcioni R, Soddu S, Davis KR, Mercurio AM** 1999 p53 inhibits $\alpha 6\beta 4$ integrin survival signaling by promoting the caspase 3-dependent cleavage of AKT/PKB. J Cell Biol 147:1063–1072
59. **Stambolic V, MacPherson D, Sas D, Lin Y, Snow B, Jang Y, Benchimol S, Mak TW** 2001 Regulation of PTEN transcription by p53. Mol Cell 8:317–325
60. **Kivela R, Silvennoinen M, Touvra AM, Lehti TM, Kainulainen H, Vihko V** 2006 Effects of experimental type 1 diabetes and exercise training on angiogenic gene expression and capillarization in skeletal muscle. FASEB J 20:1570–1572
61. **Hinton DR, Spee C, He S, Weitz S, Usinger W, LaBree L, Oliver N, Lim JI** 2004 Accumulation of NH2-terminal fragment of connective tissue growth factor in the vitreous of patients with proliferative diabetic retinopathy. Diabetes Care 27:758–764

***Endocrinology* is published monthly by The Endocrine Society (http://www.endo-society.org), the foremost professional society serving the endocrine community.**